

## Thermophoretic Depletion Follows Boltzmann Distribution

Stefan Duhr and Dieter Braun

*Applied Physics, Center for Nanoscience, Ludwig Maximilians University München, Amalienstr. 54, D-80799 München, Germany*  
(Received 26 December 2005; published 27 April 2006)

Thermophoresis, also termed thermal diffusion or the Soret effect, moves particles along temperature gradients. For particles in liquids, the effect lacks a theoretical explanation. We present experimental results at moderate thermal gradients: (i) Thermophoretic depletion of 200 nm polystyrene spheres in water follows an exponential distribution over 2 orders of magnitude in concentration; (ii) Soret coefficients scale linearly with the sphere's surface area. Based on the experiments, it is argued that local thermodynamic equilibrium is a good starting point to describe thermophoresis.

DOI: 10.1103/PhysRevLett.96.168301

PACS numbers: 82.60.Lf, 82.70.Dd, 87.23.-n

**Introduction.**—Temperature gradients can move particles, a phenomenon called the Soret effect. Experimentally, the effect has been known for 150 years [1]. Particles typically deplete from regions of enhanced temperature, but the inverted effect of thermophilic behavior is also found [2–4]. Thermophoresis is theoretically not yet understood. Experimental methods to measure thermophoresis of colloids in aqueous and nonaqueous suspensions are quite diverse and use thermal field flow fractionation (ThFFF) [5,6], beam deflection [2,4,7], holographic scattering [3,8,9], thermal lensing [10], and optical heating in microfluidics [11,12]. Thermophoresis has the potential to analyze the particle-solvent interaction of nanoscaled particles and biomolecules. Moreover, it is a versatile tool to manipulate or concentrate molecule concentrations in solution [12,13]. In addition to biotechnological applications, a natural thermophoretic setting is found in pores of rock near hot springs on the floor of the ocean, possibly involved in molecular evolution [14,15].

A generally applied assumption for describing thermophoresis is that it should be treated as a transport phenomenon using, for example, microscopic particle-particle potentials, hydrodynamics, or effective force fields [16–19]. Here, experimental evidence is presented, which explains thermophoresis for moderate temperature gradients by local thermodynamic equilibrium which diffusively connects to an exponential Boltzmann steady state distribution.

The local thermal equilibrium picture of thermophoresis leads to a scaling prediction of thermophoresis over the radius of solid particles. We confirm the prediction for polystyrene (PS) beads in water ranging from 40 nm to 2  $\mu\text{m}$  in diameter. Despite the fact that temperature is not homogeneous, our experiments argue towards a local thermodynamic equilibrium description of thermophoresis. Similar arguments have been discussed recently by Astumian [20].

**Theory.**—The process in which a temperature gradient induces a mass transport is termed thermophoresis and is described by linear phenomenological relations. Combined with diffusive back flow we find, for molecules of low

concentration [21], the drift current density

$$j = j_D + j_{TD} = -D\nabla c - D_T c \nabla T \quad (1)$$

with diffusion coefficient  $D$ , molecule concentration gradient  $\nabla c$ , thermal diffusion coefficient  $D_T$  (also termed thermophoretic mobility) and temperature gradient  $\nabla T$ . Since  $j = vc$ , the thermophoretic molecule drift velocity is linear to the temperature gradient:

$$v = -D_T \nabla T. \quad (2)$$

In the steady state, both currents compensate ( $j = 0$ ), leading to

$$\frac{dc}{c} = -S_T dT \quad (3)$$

for small temperature differences  $dT$  with the Soret coefficient  $S_T = D_T/D$ . For a constant  $S_T$ , the integration of Eq. (3) yields an exponential steady state distribution:

$$\frac{c(\vec{x})}{c_0(\vec{x}_0)} = \exp[-S_T[T(\vec{x}) - T_0(\vec{x}_0)]]. \quad (4)$$

The concentration  $c(\vec{x})$  exponentially depends on temperature  $T(\vec{x})$ . The relation is normalized by an arbitrarily defined location  $\vec{x}_0$  with a concentration  $c_0$  and temperature  $T_0$ . We experimentally test Eq. (4), made possible by a recently developed method to image thermophoresis with microfluidic fluorescence [11,12].

The exponential steady state distribution can be understood from concatenating local equilibria by diffusion. Let us consider an arbitrary division of space into smaller regions (Fig. 1) and assume that the division is sufficiently small to obtain local equilibrium in each of the regions. The ratio of end concentration  $c_N$  and start concentration  $c_0$  can be multiplied from local concentration ratios of neighboring chambers  $c_{i+1}/c_i$ , subsequently expressed by local laws of linear thermophoresis:

$$\frac{c_N}{c_0} = \prod_{i=0}^{N-1} \frac{c_{i+1}}{c_i} = \prod_{i=0}^{N-1} 1 - S_T(T_{i+1} - T_i). \quad (5)$$

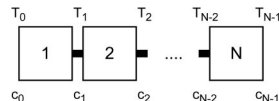


FIG. 1. Construction of a global exponential steady state by concatenation of local linear thermophoresis. At the local level, concentration ratios are proportional to temperature differences. Diffusive coupling of concentrations between local descriptions leads to a global exponential steady state distribution.

After assuming equal spacing in temperature  $\Delta T = (T_N - T_0)/N$  we can, for large  $N$ , apply the limit definition of the exponential function:

$$\frac{c_N}{c_0} = \left[ 1 - S_T \frac{T_N - T_0}{N} \right]^N \rightarrow e^{-S_T(T_N - T_0)}. \quad (6)$$

The above derivation illustrates how local thermodynamic equilibria assemble into a global exponential steady state despite nonequilibrium conditions.

*Methods.*—We used microfluidic fluorescence [11,12] to put the above exponential steady state relation to an experimental test. Temperature differences are created by an infrared laser (Furukawa FOL1405-RTV-317, 1480 nm, 25 mW) moderately focused by an aspheric lens with 8 mm focal distance (Thorlabs, C240TM-C). Water strongly absorbs at this wavelength with an attenuation length of  $\kappa = 320 \mu\text{m}$ . A 10  $\mu\text{m}$  thin water chamber was formed by polystyrene slides. Imaging was performed by a 32 $\times$  air objective (Zeiss LD-A Plan NA = 0.4) in a fluorescence upright microscope (Zeiss AxioTech) equipped with a CCD camera (PCO Sensicam QE).

Temperatures were measured by the dye BCECF used with 50  $\mu\text{M}$  concentration in 10 mM TRIS buffer [11,12] with temperature sensitivity of  $-2.8\%/\text{K}$ . The heated spot showed temperatures of  $\Delta T = 8 \text{ K}$  with a full width at half maximum of 40  $\mu\text{m}$ . We measured thermophoresis of 200 nm diameter carboxyl-modified polystyrene beads (Molecular Probes, F-8811), diluted to 0.02% solid in 1 mM Tris buffer. Their thermophoretic properties were measured for a small temperature difference of 1.2 K to  $D_T = 1.4 \mu\text{m}^2/(\text{sK})$  and  $D = 2.1 \mu\text{m}^2/\text{s}$ , yielding  $S_T = 0.7 \text{ K}^{-1}$ .

Concentration of particles was averaged from an image stack of 50 images, each with an exposure time of 10 seconds, recorded at 12-bit resolution. The imaging protocol consisted of three time steps: first without heating, second in steady state after 20 min of laser heating, and third after 20 min of backdiffusion to correct for fluorescence bleaching of the beads. Bleaching could be corrected linearly; inhomogeneous illumination was removed by dividing with the initial, unheated image stack. Radial concentration profiles were extracted from the averaged image stacks. Background fluorescence was subtracted as inferred from the central depleted region.

Several possible artifacts were excluded by the experimental design. The 32 $\times$  air objective averages the concentration profile in  $z$  direction [12]. We simulated the experiment using finite element calculations (FEMlab 2.3, Comsol) for Navier-Stokes flow superposed with heat transfer, thermal expansion, gravity, photonic momentum, molecule diffusion, and thermophoresis. The numerical approach was benchmarked previously against experiments [11,22]. The temperature profile across the chamber is flat due to the low thermal conductivity of the PS chamber walls [Fig. 2(a)]. Small deviations from a constant  $z$  profile of both temperature and concentration automatically compensate in first order [11]. The simulation does not detect a noticeable disturbance of the concentration profile by thermal convection [Fig. 2(b)]. This is understood since the latter has a maximal speed of only 5 nm/s, mostly due to the thin chamber size and the broad laser focus [Fig. 2(c)].

*Results and discussion.*—The radial temperature distribution of the heated solution was measured by BCECF fluorescence [Fig. 3(a)]. An individual image of the beads is shown in Fig. 3(b), while a logarithmic plot of the reconstructed bead concentration from the full measurement protocol is given in Fig. 3(c). Three beads which stick to the chamber surface can be seen; however, their fluorescence has no statistical significance in the final result. The remaining inhomogeneities in the center are due to insufficient averaging over the beads' movement and excluded in the analysis. Radial averages of temperature and

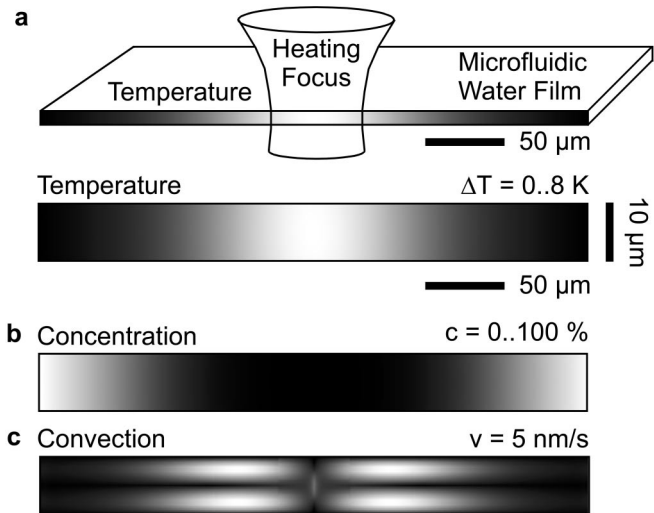


FIG. 2. Details of the experimental approach. (a) A 10  $\mu\text{m}$  thin water film is enclosed between PS walls. Low thermal conduction of the chamber walls allow a thickness independent temperature profile, confirmed by the shown finite element calculation. (b) As a result, the thermophoretic depletion profile equally shows no thickness profile. (c) Convection is slow at maximal velocities of 5 nm/s due to thin chamber and comparable broad heating focus.

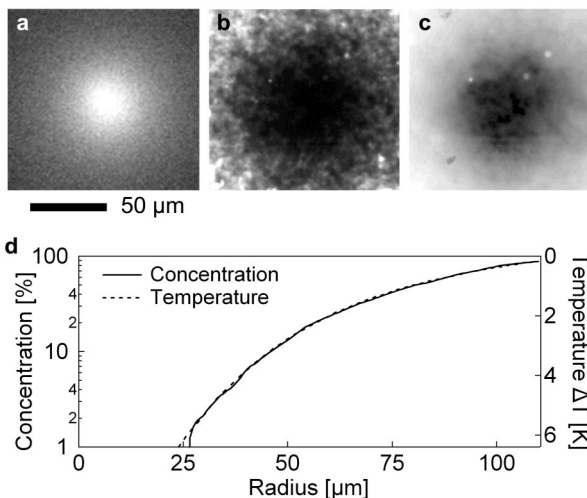


FIG. 3. Exponential thermophoretic depletion. (a) Temperature measured from BCECF fluorescence. (b) Single image of thermophoretic depleted polystyrene beads. (c) Logarithmic bead concentration image, averaged from 50 single images and after bleach and illumination correction. (d) Radial averages of particle concentration (logarithmic) and temperature (linear).

concentration are given in Fig. 3(d), notably with a logarithmic scale for concentration (left) and linear, inverted scale for temperature (right). Since both measurements correspond in the plot, we directly see that the concentration scales exponentially with temperature.

By removal of the common radius coordinate, the bead concentration is plotted over the applied temperature increase  $\Delta T$  in Fig. 4. The exponential dependence is fitted by Eq. (4) with the Soret coefficient  $S_T = 0.72/\text{K}$  (solid line) and holds well over the large concentration range from  $c/c_0 = 100\%$  down to  $1\%$ . The fitted  $S_T$  is very close to the value of  $0.7/\text{K}$  measured before at only a  $1.2\text{ K}$  elevated temperature. Carboxyl-modified polystyrene beads show a comparably low temperature dependence of

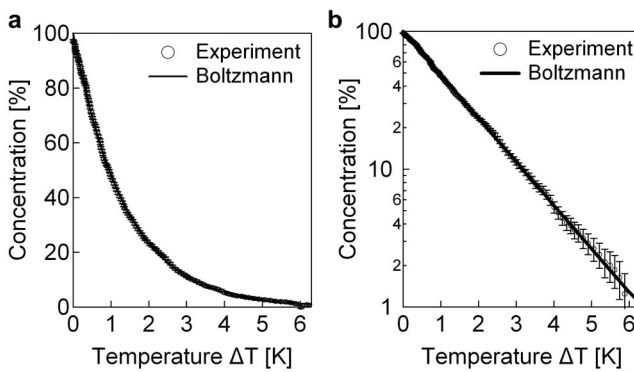


FIG. 4. Exponential concentration distribution. (a) In steady state, thermophoretic depletion results in an exponential distribution, compatible with an energetic Boltzmann distribution. (b) The logarithmic plot reveals the quality of the exponential fit over 2 orders of magnitude in concentration.

the Soret coefficient  $S_T(T) = S_T(T_0)(1 + \gamma[T - T_0])$ , measured independently to  $\gamma = 2.2\%/\text{K}$ . The experimental results can be equally described with or without above slight temperature dependence of  $S_T$ .

In hindsight, we can test the division of the nonequilibrium system into a succession of local equilibria brought forward in Eqs. (5) and (6). Locally, temperature and concentration differences are small and a linearized Boltzmann distribution holds:

$$\frac{dc}{c} = \frac{dG}{kT} = -S_T dT. \quad (7)$$

As seen, we can equate the local Boltzmann law with Eq. (3) to connect the Soret coefficient  $S_T$  with Gibbs free enthalpy  $G$ . The latter is used for the experimental condition of constant pressure and nearly constant temperature.

The finest division into local equilibria systems is limited by the finite size of the particle itself. Even at the experimentally steepest temperature gradient of  $\nabla T = 0.1\text{ K}/\mu\text{m}$ , the energy difference over the radius  $a$  of the particle is

$$a \times \nabla G = a \times S_T \nabla T kT = 0.01 kT. \quad (8)$$

The energetic asymmetry across the particle is only 2% of the particle's thermal fluctuations, which, according to Einstein [23], is  $kT/2$ . On the other side, the total energetic difference in the experiment was  $\Delta G = k\bar{T} \ln(c_{\min}/c_{\max}) = 4.6k\bar{T}$ , well beyond local equilibrium. This means that the partitioning introduced in Eqs. (5) and (6) and Fig. 1 can be applied with at least  $N = 4.6/0.01 = 460$ , yielding a well converged exponential steady state distribution in Eq. (6).

Based on experimental evidence, it is tempting and along the lines of Astumian [20] to describe thermophoretic steady states by a Boltzmann distribution for cases where local thermodynamic equilibrium can be assumed:

$$\frac{c}{c_0} = \exp[-S_T(T - T_0)] = \exp\left[-\frac{G(T) - G(T_0)}{k\bar{T}}\right]. \quad (9)$$

The linear relation between the Soret coefficient  $S_T$  and particle energy  $G$  in Eq. (7) leads to a scaling prediction of thermophoresis over particle size. For solid particles, only the solvation energy at their surface can be temperature dependent. Therefore, based on Eq. (7), the Soret coefficient must scale with particle surface area. Since  $D \propto a^{-1}$ ,  $D_T$  scales with a particle radius:

$$S_T \propto \frac{\partial G}{\partial T} \propto a^2, \quad D_T \propto D \frac{\partial G}{\partial T} \propto a. \quad (10)$$

We measured Soret coefficients for carboxyl-modified polystyrene beads of various size (Molecular Probes, F-8888, F-8823, F-8827, F-8795, and F-8823) in 1 mM TRIS buffer. Measurements for beads larger than 200 nm in diameter were obtained from single particle tracking [24]. The measurements are well fitted with the scaling

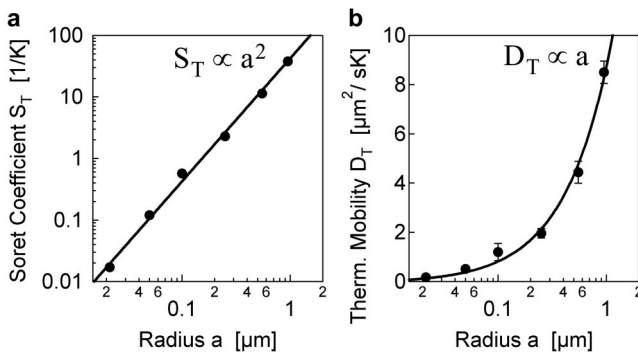


FIG. 5. Scaling of the Soret coefficient  $S_T$  and thermophoretic mobility  $D_T$  with particle size. (a) The Soret coefficient of carboxyl-modified beads of different radius  $a$  scale with its particle surface area, confirming a local equilibrium description of thermophoresis. (b) Accordingly, thermophoretic diffusion coefficient  $D_T$  scales linearly with radius.

of Eq. (10) (Fig. 5, solid lines). Hydrodynamic theories [16–19] predict particle-size independent  $D_T$  and thus  $S_T \propto a$ , in contradiction to the experimental data.

Similar particle-solvent systems have been analyzed with ThFFF [5,6]. ThFFF uses exceptionally strong thermal gradients of up to 1 K/μm and leads to values for  $S_T$  and  $D_T$  for small polystyrene beads that are comparable to our measurements. However, for larger particles in ThFFF, the energetic difference of Eq. (8) exceeds  $kT$  and local equilibrium cannot be assumed. This transition, given by  $a \times S_T \Delta T = 1$  strongly depends on particle size ( $\nabla T \propto a^{-3}$ ) due to Eq. (10). Incidentally, measurements of ThFFF versus particle size, typically for diameters between 50 and 400 nm, are performed near the transition. Often, saturation of retention times  $t_R/t_0$  over particle radius is found and results in a hard to explain scatter in size scaling laws for different particle systems [5,6] and in contradiction to our results.

Based on recent findings [24], the contradiction, however, can be readily resolved. We find using single particle tracking that the linearity  $v = -D_T \nabla T$  does not hold out of local equilibrium. The relation saturates nonlinearly for larger thermal gradients. Since evaluations of ThFFF assume a linear transport relation, apparent values for  $D_T$  and  $S_T$  decrease beyond the transition. This probably leads to the discrepancy of size scaling measured with ThFFF and our method (Fig. 5), where considerable smaller thermal gradients were used to ensure local equilibrium.

To conclude, we collected experimental evidence in favor of describing thermophoresis by local thermodynamic equilibrium. Under moderate thermal gradients, thermophoretic depletion follows an exponential steady state distribution over 2 orders of magnitude. Identification with a

local Boltzmann distribution leads to a scaling law of the Soret coefficient for solid particles, which is confirmed experimentally, but contradicts hydrodynamic transport models of thermophoresis [16–19].

We thank Jan Dhont, Werner Köhler, and Simone Wiegand for discussions and Hermann Gaub for hosting our Emmy-Noether Group which was funded by the Deutsche Forschungsgemeinschaft DFG.

- [1] C. Ludwig, Sitzber. Kaiserl. Akad. Wiss. Math.-Naturwiss. Kl. (Wien) **20**, 539 (1856).
- [2] M. Giglio and A. Vendramini, Phys. Rev. Lett. **38**, 26 (1977).
- [3] B.-J. de Gans, R. Kita, B. Müller, and S. Wiegand, J. Chem. Phys. **118**, 8073 (2003).
- [4] S. Iacopini and R. Piazza, Europhys. Lett. **63**, 247 (2003).
- [5] S. J. Jeon, M. E. Schimpf, and A. Nyborg, Anal. Chem. **69**, 3442 (1997).
- [6] P. M. Shiundu, G. Liu, and J. C. Giddings, Anal. Chem. **67**, 2705 (1995).
- [7] R. Piazza and A. Guarino, Phys. Rev. Lett. **88**, 208302 (2002).
- [8] J. Rauch and W. Köhler, Phys. Rev. Lett. **88**, 185901 (2002).
- [9] S. Wiegand and W. Köhler, in *Thermal Nonequilibrium Phenomena in Fluid Mixtures* (Springer, Berlin, 2002), p. 189.
- [10] R. Rusconi, L. Isa, and R. Piazza, J. Opt. Soc. Am. B **21**, 605 (2004).
- [11] S. Duhr, S. Arduini, and D. Braun, Eur. Phys. J. E **15**, 277 (2004).
- [12] D. Braun and A. Libchaber, Phys. Rev. Lett. **89**, 188103 (2002).
- [13] A. Voit, A. Krekhov, W. Enge, L. Kramer, and W. Köhler, Phys. Rev. Lett. **94**, 214501 (2005).
- [14] Dieter Braun and Albert Libchaber, Physical Biology **1**, P1 (2004).
- [15] Dieter Braun, Noel L. Goddard, and Albert Libchaber, Phys. Rev. Lett. **91**, 158103 (2003).
- [16] K. I. Morozov, J. Exp. Theor. Phys. **88**, 944 (1999).
- [17] M. E. Schimpf and S. N. Semenov, J. Phys. Chem. B **105**, 2285 (2001).
- [18] A. Parola and R. Piazza, Eur. Phys. J. E **15**, 255 (2004).
- [19] J. R. Bielenberg and H. Brenner, Physica (Amsterdam) **356A**, 279 (2005).
- [20] R. D. Astumian, Am. J. Phys. (to be published).
- [21] S. R. de Groot and P. Mazur, *Non-Equilibrium Thermodynamics* (North-Holland, Amsterdam, 1962).
- [22] S. Duhr and D. Braun, Appl. Phys. Lett. **86**, 131921 (2005).
- [23] A. Einstein, Ann. Phys. (Berlin) **22**, 569 (1907).
- [24] S. Duhr and D. Braun (to be published).